NASA Technical Memorandum 109080

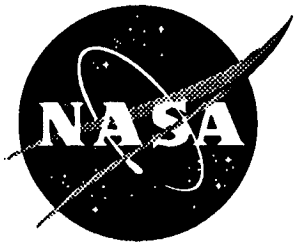

# The Relationship of an Integral Wind Shear Hazard to Aircraft Performance Limitations

M. S. Lewis, P. A. Robinson, D. A. Hinton, and R. L. Bowles
*Langley Research Center, Hampton, Virginia*

February 1994

National Aeronautics and
Space Administration
Langley Research Center
Hampton, Virginia 23681-0001

# The Relationship of an Integral Wind Shear Hazard to Aircraft Performance Limitations

M. S. Lewis, P. A. Robinson, D. A. Hinton, and R. L. Bowles

**Abstract**

The development and certification of airborne forward-looking wind shear detection systems has required a hazard definition stated in terms of sensor observable wind field characteristics. This paper outlines the definition of the F-factor wind shear hazard index and an average F-factor quantity, $\overline{F}$, calculated over a specified averaging interval, which may be used to judge an aircraft's potential performance loss due to a given wind shear field. A technique for estimating airplane energy changes during a wind shear encounter is presented and used to determine the wind shear intensity, as a function of the averaging interval, that presents a significant hazard to transport category airplanes. The wind shear hazard levels are compared to $\overline{F}$ values at various averaging intervals for four actual wind shear encounters. Results indicate that averaging intervals of about 1 kilometer could be used in a simple method to discern hazardous shears.

## 1 Nomenclature

| | |
|---|---|
| $D$ | aircraft drag |
| $E$ | aircraft total energy: kinetic energy + potential energy |
| $E'$ | aircraft specific total energy |
| $\tilde{e}_a$ | airspeed unit vector |
| $F$ | F-factor |
| $\overline{F}$ | averaged F-factor |
| $g$ | acceleration due to gravity |
| $h$ | height above ground |

| | |
|---|---|
| $m$ | mass of aircraft |
| $V_a$ | airspeed |
| $\dot{\underline{W}}_I$ | time rate of change of inertial wind vector $\underline{W}_I$ |
| $W_z^I$ | vertical component of the inertial wind (positive down) |
| $w$ | aircraft weight = $mg$ |

# 2 Introduction

The development of airborne forward-looking wind shear detection systems and their certification standards has required that the wind shear hazard be defined. Characteristics of the required definition include compatibility with existing reactive detection systems and crew training, that aircraft performance limitations be considered, and that the definition parameters be quantifiable by remote sensors. Existing reactive detection systems utilize the F-factor hazard index, suitably filtered for gust rejection (Reference 1). This paper outlines the definition of the F-factor wind shear hazard index, the derivation of the components contributing to the magnitude of the F-factor, and the development of a quantity $\overline{F}$ which may be used to judge the aircraft performance loss potential of a given wind shear field. The $\overline{F}$ quantity may then be used to determine appropriate wind shear alerting thresholds following the definition of acceptable aircraft airspeed and height loss and a number of other important variables.

# 3 Hazard Index Development

## 3.1 The F-Factor Definition

A full description of the F-factor, its implementation and its use, can be found in Reference 1. An abbreviated description is included herein.

The total specific energy of an aircraft (relative to the airmass) is given by

$$\frac{E}{m} = E' = \frac{V_a^2}{2g} + h \tag{1}$$

and its rate of change by

$$\dot{E}' = \frac{V_a \dot{V}_a}{g} + \dot{h} \tag{2}$$

Incorporating wind terms into the aircraft wind axis equations of motion, the rate of change of specific energy can also be shown to be

$$\dot{E}' = V_a \left( \frac{T - D}{w} - F \right) \tag{3}$$

where the F-factor wind shear index, $F$, is defined as

$$F = \frac{\dot{\underline{W}}_I \cdot \tilde{\underline{e}}_a}{g} + \frac{W_z^I}{V_a} \tag{4}$$

The first term in the F-factor is the dot product of the derivative of the inertial wind vector and a unit vector along the aircraft airspeed vector divided by the acceleration of gravity. The second term is the local inertial vertical wind speed divided by aircraft airspeed.

The F-factor describes the rate at which the wind field changes the energy of the aircraft. A negative value of F is produced by a performance increasing wind shear such as an increasing headwind or updraft (or a combination of the two), and a positive value of F by a performance decreasing shear such as a decreasing headwind or downdraft (or a combination of the two). An aircraft experiencing a wind shear with an F-factor of 0.1 must produce a $(T - D)/w$ (or specific excess thrust) ratio of 0.1 in order to maintain level flight at constant speed. Conversely, a performance increasing shear of -0.1 F-factor requires a specific excess thrust reduction to maintain steady flight. Importantly for large magnitude wind shears, an F-factor value which exceeds the maximum specific excess thrust performance of an aircraft will force that aircraft to lose some combination of airspeed or altitude regardless of pilot input. For reference, a typical twin-engine commercial transport may have a maximum specific excess thrust performance of approximately 0.17, a typical three-engine aircraft 0.13, and a typical four-engine aircraft 0.11. All values are for maximum available thrust in a clean configuration at the aircraft's maximum gross weight. The values may vary depending on the aircraft type and configuration, however these numbers provide a useful illustration of the calculation technique as well as a quantification of the relative effects of wind shear among two-, three-, and four-engine transport aircraft.

## 3.2 The $\overline{F}$ Index

Reactive systems, which cannot predict the scale length of a wind shear, must rely on in situ measurements of the F-factor and apply gust rejection filters to minimize nuisance alerts. Forward-looking systems provide the capability to determine the spatial extent of a wind shear prior to the encounter. This additional information may be used to compute a hazard index that scales with the aircraft's performance and energy margins. However the F-factor is proportional to the time rate of change of specific energy as shown in Equation (3). Therefore the aircraft's temporal net energy loss or gain must be related to the measured spatial variations of F.

Combining Equations (2) and (3) gives

$$V_a\left(\frac{T-D}{w}-F\right) = \frac{V_a\dot{V}_a}{g}+\dot{h} \tag{5}$$

The measured quantities $V_a$, $\dot{V}_a$, and $\dot{h}$, are functions of time and may be transformed from temporal variations to spatial variations calculated along the flight path, $s$. For level flight

$$\dot{E}' = \frac{\partial E'}{\partial t} = \frac{\partial E'}{\partial s}\frac{\partial s}{\partial t} = V_g\frac{\partial E'}{\partial s} \tag{6}$$

from Equation (3)

$$\frac{\partial E'}{\partial s} = \frac{V_a}{V_g}\left(\frac{T-D}{w}-F\right) \tag{7}$$

Airspeed and inertial groundspeed are related by (for level flight)

$$\vec{V}_g = \vec{V}_a + \vec{W} \tag{8}$$

By relating the relative magnitudes, it can be shown that for small flight path angles ($\gamma_w$)

$$\frac{V_a}{V_g} = 1 - O\left(\frac{W}{V_g}\right) \tag{9}$$

At points within a wind shear the second term in this approximation may be significant, but on integrating over the length of a headwind/tailwind shear the approximation will hold. Therefore the approximation can be made

$$\frac{\partial E'}{\partial s} = \left(\frac{T-D}{w} - F\right) \tag{10}$$

Integrating from a point in space, $s_o$, over some interval $L$ gives

$$\Delta E'(s_o, L) = \int_{s_o}^{s_o+L} \left(\frac{T-D}{w}\right) ds - \int_{s_o}^{s_o+L} F ds \tag{11}$$

From Equation (1) the total net energy change experienced by an aircraft passing through this region of shear (between $s_o$ and $s_o + L$) is given by

$$\begin{aligned} \Delta E' &= E_{s_o+L} - E_{s_o} \\ &= \left(\frac{V_a^2}{2g} + h\right)_{s_o+L} - \left(\frac{V_a^2}{2g} + h\right)_{s_o} \end{aligned} \tag{12}$$

or

$$\Delta E'(s_o, L) = \frac{\Delta(V_a^2)}{2g} + \Delta h \tag{13}$$

where $\Delta(V_a^2) = (V_a^2)_{s_o+L} - (V_a^2)_{s_o}$. Combining Equations (11) and (13) gives

$$\int_{s_o}^{s_o+L} \left(\frac{T-D}{w}\right) ds - \int_{s_o}^{s_o+L} F ds = \frac{\Delta(V_a^2)}{2g} + \Delta h \tag{14}$$

and

$$\int_{s_o}^{s_o+L} F ds = \int_{s_o}^{s_o+L} \left(\frac{T-D}{w}\right) ds - \frac{\Delta(V_a^2)}{2g} - \Delta h \tag{15}$$

Defining the averaged integral quantity

$$\bar{F}(s_o, L) = \frac{1}{L} \int_{s_o}^{s_o + L} F ds \tag{16}$$

gives

$$\bar{F}(s_o, L) = \frac{1}{L} \int_{s_o}^{s_o + L} \left( \frac{T - D}{W} \right) ds - \frac{\Delta (V_a^2)}{2gL} - \frac{\Delta h}{L} \tag{17}$$

$\bar{F}(s_0, L)$ represents an equivalent average F-factor over some interval L, starting at position $s_0$.

# 4 Applications

## 4.1 Takeoff and Landing Performance

The first application of Equation (17) will be to determine the typical wind shear penetration performance capabilities of two-, three-, and four-engine transport aircraft. Given specific energy input conditions, and an allowable energy loss, it is possible to determine the magnitude and the spatial extent of $\bar{F}$ along the flight path which an aircraft can withstand.

The expression for $\bar{F}(s_0, L)$ in Equation (17) may be used to determine the average wind shear intensities which, given a certain thrust response, will produce a specified performance loss expressed in terms of airspeed and altitude losses. In order to do this, assumptions must be made in the variation of $(T - D)/w$ corresponding to a pilot recognizing the wind shear encounter, and responding to it by applying thrust. For takeoff it is assumed that the aircraft engines are developing full power and the thrust is constant throughout the wind shear encounter. For an approach along a glideslope, the engines may be throttled back and the pilot's response time to the onset of wind shear and the engines' spool up time must be taken into account. A representative profile of $(T - D)/w$ variation for wind shear encounters on landing is shown in Figure 1.

Table 1 gives the parameters used in the calculation of $\bar{F}$. The calculation begins at the beginning of the wind shear event, therefore $s_0 = 0$ (and in Figure 1, t = 0 represents the beginning of the event). The allowable airspeed loss in each case represents typical margins to stick shaker activa-

tion, and the allowable height loss is a postulated maximum acceptable worst case value. For a given value of the interval $L$ the first term on the right hand side of Equation (17) is evaluated by determining the time elapsed since the beginning of the event using the initial airspeed $(t = L/V_a)$ [1], and integrating under the curve in Figure 1 from $t = 0$ up to $t = L/V_a$. The other two terms in Equation (17) are calculated simply from the appropriate values given in Table 1.

The results are shown in Figure 2. At intervals of less than about 500 m, extremely high $\overline{F}$ values are required for the limiting energy loss. At such short values of L, the curves for all aircraft types merge, suggesting that the individual aircraft performance characteristics do not greatly influence the energy losses. This result is strongest in the landing scenario, since the $(T-D)/w$ ratio is identical for all aircraft on the glideslope, and a finite time and distance is required to increase thrust. At interval values of 1 km, individual aircraft characteristics are apparent and the worst-case aircraft situation requires an $\overline{F}$ of 0.12 for limiting performance. Beyond 1 km, the curves rapidly asymptote to values close to the 1 km value. An exception is the two-engine landing scenario. At short intervals the engine spool-up is not completed while in the shear, lowering performance. At longer values the spool-up is completed well before exiting the shear, and the full performance capabilities of the aircraft are utilized. The engine spool-up factor is much less pronounced in the three- and four-engine cases, as the maximum performance of the airplane is essentially the same as the 1 km limiting $\overline{F}$ value. Note that the curves in Figure 2 represent results for the worst case low-altitude encounter. Much higher $\overline{F}$ values could be sustained given higher initial energy conditions.

It is possible to relate the interval L to typical atmospheric phenomena in a general sense. High levels of $\overline{F}$ over short distances (up to 400 m) may be experienced as turbulence. Longer shear lengths (400 - 4000m) may be the results of microbursts, gust fronts, or other associated phenomena. Larger shear length (over 4000m) events may exist in the atmosphere but rarely at the levels shown to be hazardous to an aircraft.

Note that for a given thrust profile, $\overline{F}$ values calculated are a function of initial and final airspeed and height conditions only. The energy loss an aircraft experiences due to a shear over a given distance is a function of the integral of the instantaneous shear values. No unique spatial distribution of that shear is required in these calculations. Due to the non-linearity of Equation (5) (and

1. In fact in a wind shear encounter the airspeed and groundspeed are changing and not necessarily equal. The fact that the initial airspeed is used in the space/time conversion illustrates that this is an approximation to a non-linear problem.

the consequent non-linearity of Equation (17)) several such simplifying assumptions had to be made. These assumptions, effectively linearizing the problem, allow a first approximation to the wind shear hazard threat definition to be made. A more complex analysis procedure than presented above would be required to evaluate the full non-linear problem. Similar energy analysis techniques have been used in the past, however, and compared with non-piloted simulation results obtained from a point-mass, Boeing 737 model that incorporated realistic lift and drag changes with angle of attack (Reference 2). In that study the simulation results were consistent with the energy analysis. Results from the point mass Boeing 737 model have also compared well with full six degree of freedom, non-linear, piloted simulation study results (Reference 3).

4.2 Wind Shear Case Studies

The curves generated in Section 4.1 define an aircraft's performance capability in the presence of energy losses and can be related directly to values of $\overline{F}$ from atmospheric measurements. The curves do not, however, provide guidance on the scale lengths of real wind shear events that should be used in threat determination. This section presents $\overline{F}$ as a function of averaging interval for four actual wind shear encounters by aircraft to provide insight on those scale lengths that can discriminate true threats.

Calculation Method

A discrete spatial series of $F$, $\{F_n\}$, may be obtained from on-board flight data recordings (converted from time series) consisting of $N$ points equally spaced by $\Delta r$, $(n = 1, 2, \ldots, N)$. For a particular value of $L$ (the averaging interval), discrete values of $\overline{F}(s_o, L)$ are calculated using a discretized form of Equation (16)

$$\{\overline{F}_j(L)\} = \frac{1}{N_{ave}} \sum_{j=m}^{m+N_{ave}} F_j \qquad m = 1, 2, \ldots, (N - N_{ave}) \tag{18}$$

where $N_{ave} = L/(\Delta r)$. The resulting series, $\{\overline{F}_j(L)\}$, is a moving average over $N_{ave}$ points, starting at the beginning of the series, $F_1$, and ending at $F_{N-N_{ave}}$. The value of interest (worst case shear) for a given averaging interval L is the maximum value of $\overline{F}$ in this series. This value may be compared to the aircraft performance curves of Figure 2. This method is now applied to four actual wind shear encounters.

Case 1

A Boeing 737 aircraft on final approach to Denver Stapleton Airport which penetrated a microburst and descended below 100 feet AGL well short of the runway threshold prior to establishing a positive rate of climb and recovery (Reference 4). The values of $\overline{F}$ calculated from the flight data recorder for this event is compared to a typical 2 engine landing performance curve in Figure 3.

Case 2

A Boeing 767 aircraft on final approach to Atlanta Hartsfield Airport which penetrated a microburst and descended to approximately 70 feet AGL short of the runway threshold prior to establishing a positive rate of climb and successful missed-approach. As in Case 1, the $\overline{F}$ curve calculated from the flight recorder data is compared with a typical 2 engine aircraft performance curve and is shown in Figure 4.

Case 3

A Lockheed L-1011 aircraft which crashed while on the approach to Dallas-Ft. Worth Airport in May 1985 (Reference 5). The aircraft entered a microburst while at approximately 750 feet AGL and was not able to recover. The derived curves are shown in Figure 5.

Case 4

NASA's Boeing 737 research aircraft which deliberately penetrated a microburst at approximately 900 feet AGL near Orlando FL. in June 1991 (Reference 6). Figure 6 shows the $\overline{F}$ curves for this event as well as the appropriate 2 engine performance curve. A description of the NASA research flight program is found in Reference 7.

Also included in the figures is an alert threshold boundary specified for reactive detection systems (Reference 8). As can be seen from the figures, all the above cases were of large enough magnitude to warrant an alert. Case 3 was clearly more severe than the other three cases. Assuming a specific excess thrust performance capability for the L-1011 of 0.15, this microburst shear exceeded the aircraft's ability to maintain level flight for nearly three kilometers, or nearly 40 seconds of flight time.

As can be seen from these case studies, the $\overline{F}$ value of real events varies significantly with the averaging interval chosen. Every event shown had a significant $\overline{F}$ value at very short averaging

intervals, although not always in excess of the aircraft performance limit curve. Averaging intervals less than about 500 m would be a poor choice for discriminating threats due to the presence of turbulence and the poor comparison with aircraft performance. Reactive detection systems are designed to reject such small scale motion even with $\overline{F}$ values in excess of 0.2. Beyond averaging intervals of 1.5 to 3.5 km, $\overline{F}$ values fall below the reactive detection thresholds. Even large scale, severe events such as the Dallas - Fort Worth microburst do not sustain shears over greater averaging intervals than about 3 to 4 km. Averaging intervals greater than about 1.5 km to 2 km would also be a poor choice for a detection system, as threatening events of small spatial extent may produce very low $\overline{F}$ values at these averaging intervals. In each case study, the $\overline{F}$ value exceeded both the reactive threshold and the aircraft performance limit curve at averaging intervals near 1 km.

## 5 Concluding Remarks

The analysis presented above provides a suitable parameter, $\overline{F}$, for quantification of the wind shear hazard by forward-looking sensors, as well as a method of establishing a hazard definition for systems requirements and certification testing. Given aircraft performance characteristics, microburst encounter geometry, and a minimum allowable aircraft energy at microburst exit, a limiting $\overline{F}$ value may be found which will produce the specified exit energy. The energy analysis employed does not model all factors that are involved in a wind shear recovery, such as the piloting technique used to trade altitude for airspeed or the variation of F-factor with varying paths, but does provide a first-order approximation to the survivability of a particular wind shear encounter. The analysis has both conservative and non-conservative factors. The results are conservative in that the performance-increasing shear, usually encountered prior to hazardous wind shears, is not modeled. This initial performance increase would provide additional energy for the recovery, and is particularly important in very small scale events, such as turbulence, where the aircraft crosses performance-decreasing regions and reenters performance-increasing regions before any significant flight path change can occur. This effect is not modeled and results in artificially low values of limiting $\overline{F}$ at short averaging intervals. The allowable energy loss values used in this analysis also effectively place the microburst in the worst-case location for landing and departure. Any other location would increase survivability. The results can be made even more conservative by assuming lower aircraft performance, longer engine spool-up time or pilot delay, or a higher

required minimum energy. The results are non-conservative in that adequate airplane performance for recovery does not guarantee survival, given variances in pilot technique. This effect may be minimized by specifying ample exit energy, particularly in the airspeed margins.

Comparison of the performance limit curves with estimated $\overline{F}$ values from a variety of real events suggests that the best simple discriminator of a hazard is $\overline{F}$ taken at an averaging interval near 1 kilometer. Lower averaging intervals will be dominated by turbulence, which is not a performance threat, and higher averaging intervals may result in very low $\overline{F}$ values for hazardous events that would activate an installed reactive detection system. In each case studied, the hazardous wind shear event exceeded the appropriate aircraft performance limit curve at scale lengths near 1 kilometer.

The analysis presented here may be used to derive forward-look sensor certification requirements and establish reasonable hazard thresholds, when combined with appropriate takeoff and landing configuration airplane performance characteristics, and minimum energy requirements acceptable to the FAA and the aviation community.

## 6 References

1. Oseguera, R. M., Bowles, R. L., and Robinson, P. A., "Airborne In Situ Computation of the Wind Shear Hazard Index", AIAA 92-0291, 30th Aerospace Sciences Meeting, Reno, NV., January 6-9 1992.

2. Hinton, David A., " Relative Merits of Reactive and Forward-Look Detection for Wind-Shear Encounters During Landing Approach for Various Microburst Escape Strategies", NASA TM 4158, DOT/FAA/DS-89/35, February, 1990.

3. Hinton, D.A., "Forward-Look Wind Shear Detection for Microburst Recovery", Journal of Aircraft, Vol. 29, No 1, Jan-Feb 1992, pp. 63-66.

4. Schlickenmaier, Herbert W., "Windshear Case Study: Denver, Colorado, July 11, 1988", DOT/FAA/DS-89/19, November 1989.

5. National Transportation Safety Board, Aircraft Accident Report, Delta Air Lines, Inc., Lockheed L-1011-385-1, N726DA, Dallas/Fort Worth - International Airport, Texas, August 2, 1985, NTSB/AAR-86/05, August 1986.

6. Oseguera, R. M., "NASA Wind Shear Flight Test In Situ Results", NASA CP 10105 part 1 DOT/FAA/RD-92/19-I pp 45-58, Fourth Combined Manufacturers' and Technologists' Conference, September 1992.

7. Lewis, M. S., Yenni, K. R., Verstynen, H. A., and Person; L. H., "Design and Conduct of a Flight Experiment to Detect and Penetrate Microburst Windshears in a Transport Category Aircraft", AIAA 6th Biennial Flight Test Conference, Hilton Head, SC, August 24-26, 1992, AIAA 92-4092.

8. Federal Aviation Administration, Airborne Windshear Warning and Escape Guidance Systems for Transport Airplanes, Technical Standard Order C117, July 24, 1990.

| | | Take-off | Landing |
|---|---|---|---|
| $(T-D/w)_{min}$: | (all aircraft) | $(T-D/w)_{max}$ | -0.0524 (-3°) |
| $(T-D/w)_{max}$: | 2-engine aircraft | 0.17 | 0.17 |
| | 3-engine aircraft | 0.13 | 0.13 |
| | 4-engine aircraft | 0.11 | 0.11 |
| $t_p$ [sec] | | 0 | 5 |
| $t_e - t_p$ [sec] | | 0 | 5 |
| Initial airspeed [kts]: | 2-engine aircraft | 125 | 140 |
| | 3-engine aircraft | 135 | 150 |
| | 4-engine aircraft | 145 | 160 |
| Allowed airspeed loss [kts] | | 15 | 25 |
| Allowed height loss [ft] | | 0 | 50 |

Table 1: Parameters for Hazard Limit Calculations

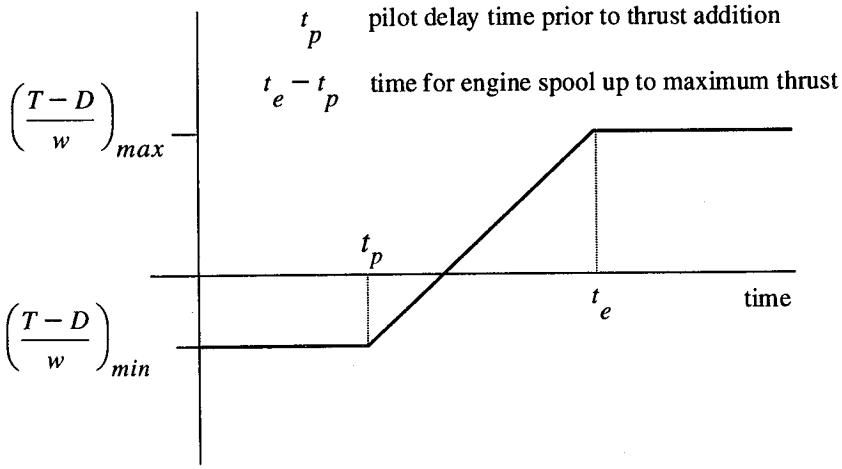


Figure 1 : Representative Energy Profile for $\overline{F}$ Calculations

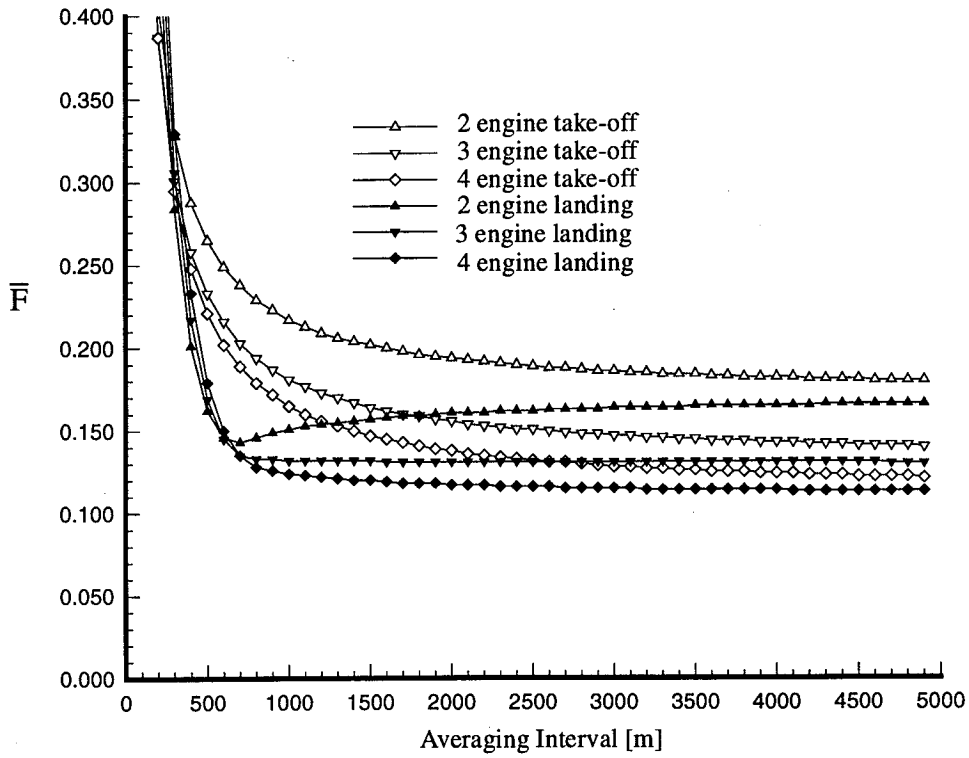


Figure 2 : Aircraft Performance Curves

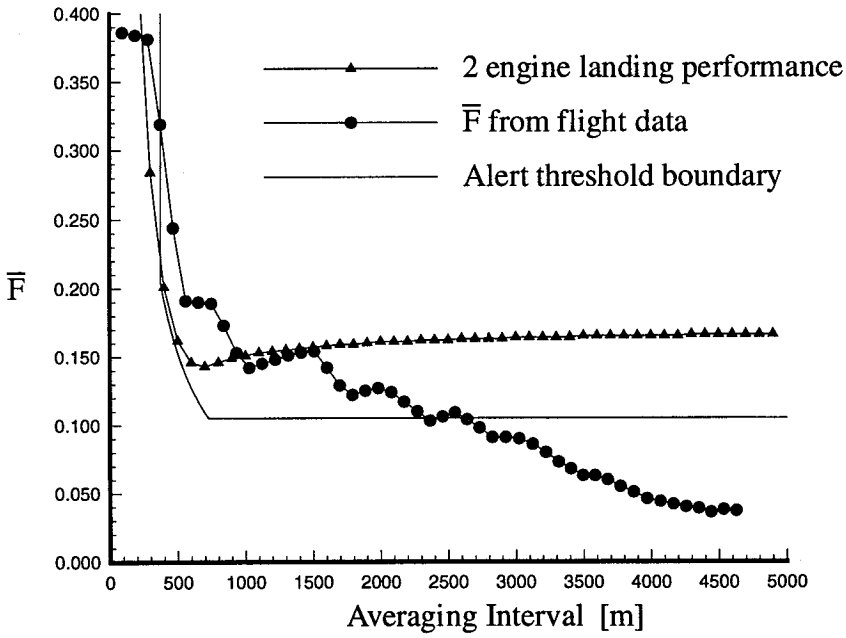


Figure 3 : Case 1 Data

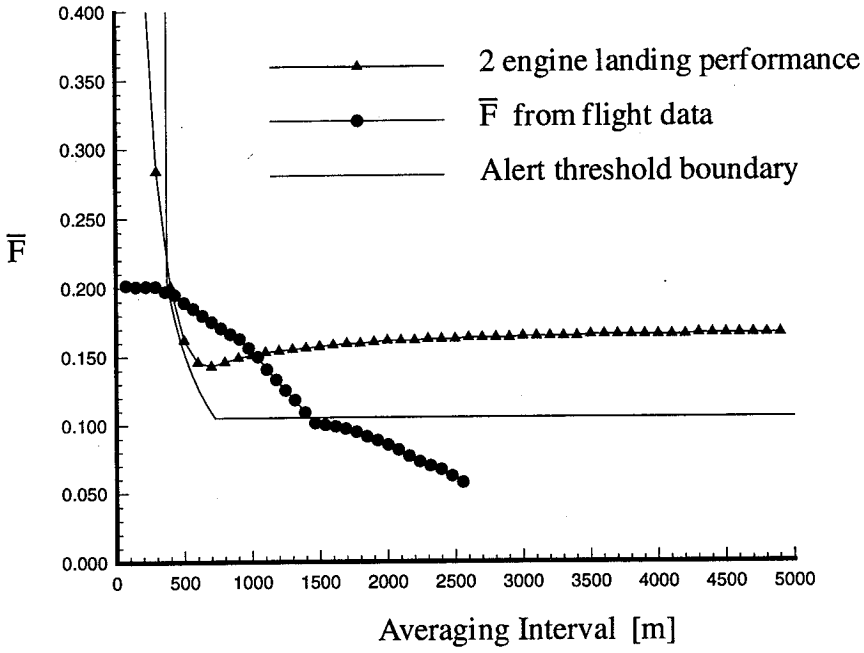


Figure 4 : Case 2 Data

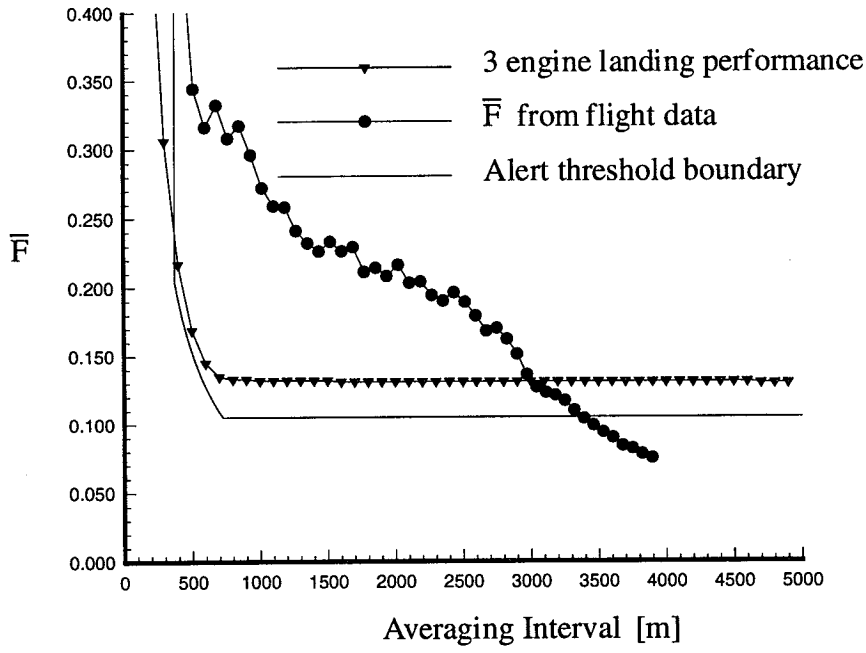


Figure 5 : Case 3 Data

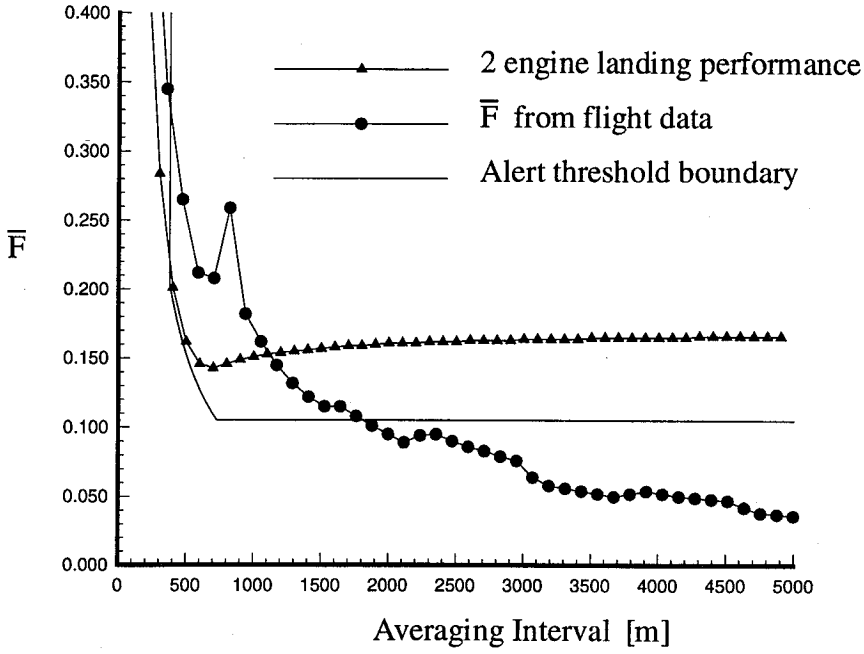


Figure 6 : Case 4 Data

# REPORT DOCUMENTATION PAGE

*Form Approved*
*OMB No. 0704-0188*



| 1. AGENCY USE ONLY (*Leave blank*) | 2. REPORT DATE | 3. REPORT TYPE AND DATES COVERED |
|---|---|---|
| | February 1994 | Technical Memorandum |

**4. TITLE AND SUBTITLE**
The Relationship of an Integral Wind Shear Hazard to Aircraft Performance Limitations

**5. FUNDING NUMBERS**
505-64-12-01

**6. AUTHOR(S)**
M. S. Lewis, P. A. Robinson, D. A. Hinton, and R. L. Bowles

**7. PERFORMING ORGANIZATION NAME(S) AND ADDRESS(ES)**
NASA Langley Research Center
Hampton, VA 23681-0001

**8. PERFORMING ORGANIZATION REPORT NUMBER**

**9. SPONSORING / MONITORING AGENCY NAME(S) AND ADDRESS(ES)**
National Aeronautics and Space Administration
Washington, DC 20546-0001

**10. SPONSORING / MONITORING AGENCY REPORT NUMBER**
NASA TM-109080

**11. SUPPLEMENTARY NOTES**

**12a. DISTRIBUTION / AVAILABILITY STATEMENT**
Unclassified - Unlimited
Subject Category 08

**12b. DISTRIBUTION CODE**

**13. ABSTRACT** (*Maximum 200 words*)

The development and certification of airborne forward-looking wind shear detection systems has required a hazard definition stated in terms of sensor observable wind field characteristics. This paper outlines the definition of the F-factor wind shear hazard index and an average F-factor quantity, calculated over a specified averaging interval, which may be used to judge an aircraft's potential performance loss due to a given wind shear field. A technique for estimating airplane energy changes during a wind shear encounter is presented and used to determine the wind shear intensity, as a function of the averaging interval, that presents significant hazard to transport category airplanes. The wind shear hazard levels are compared to averaged F-factor values at various averaging intervals for four actual wind shear encounters. Results indicate that averaging intervals of about 1 kilometer could be used in a simple method to discern hazardous shears.

| 14. SUBJECT TERMS | 15. NUMBER OF PAGES |
|---|---|
| Wind Shear; Microburst; Aircraft Performance | 17 |
| | 16. PRICE CODE: A03 |

| 17. SECURITY CLASSIFICATION OF REPORT | 18. SECURITY CLASSIFICATION OF THIS PAGE | 19. SECURITY CLASSIFICATION OF ABSTRACT | 20. LIMITATION OF ABSTRACT |
|---|---|---|---|
| Unclassified | Unclassified | | |